

Resonant acoustic modes at a liquid-⁴He–copper interface

K. N. Zinov'eva, D. A. Narmoneva, and A. S. Semenov

P. A. Kapitsa Institute of Physics Problems, Russian Academy of Sciences, 117973 Moscow, Russia

(Submitted 12 January 1994)

Zh. Eksp. Teor. Fiz. **105**, 1280–1310 (May 1994)

Calculations and measurements of the transmission of acoustic energy through a ⁴He–copper single crystal interface at frequencies in the range 13–300 MHz and temperatures in the range 100–400 mK were performed. The resonant transmission of phonons in the presence of interaction with a pseudosurface wave was observed experimentally. The effect of anisotropy on the energy transmission coefficient of resonant surface modes—Rayleigh and pseudosurface waves—was investigated. It is shown that the dissipative acoustic theory agrees quantitatively with the experimental results. The degeneration of a surface wave into a volume wave near the [110] direction on the (001) plane of copper was investigated.

1. INTRODUCTION

1.1. Kapitsa resistance problem

Thermal boundary resistance was first investigated by Kapitsa in 1941 in a study of the heat flux near a copper sample in liquid helium.¹ The discovery of boundary resistance led to a large number of theoretical and experimental works. We call attention especially to Khalatnikov's work,² where a theoretical model was first proposed for this phenomenon. This model is now known as the acoustic mismatch model (AMM). According to the AMM, the heat flux \dot{Q} through an interface leads to a finite jump in the temperature between the media (Kapitsa jump), the temperature difference ΔT being proportional to this flux:

$$\Delta T = \frac{R_K}{S} \dot{Q}. \quad (1)$$

Here S is the contact area of the two media and R_K is the coefficient of proportionality, known as the Kapitsa resistance. In calculations it is more convenient to employ the reciprocal of R_K , known as the Kapitsa conductance $h_K = 1/R_K$:

$$\dot{Q} = S h_K \Delta T. \quad (2)$$

In the theoretical works mentioned above, the Kapitsa resistance R_K at 1 K is estimated to be $10^3 \text{ K} \cdot \text{cm}^2/\text{W}$, and it is predicted that R_K increases with decreasing temperature as T^{-3} . This is a very important result: it implies that heat removal at low temperatures is strictly limited and that the time required to establish thermal equilibrium increases rapidly.

1.2. Basic tenets of the AMM

It is assumed that heat is transferred by phonons incident on the interface from both sides. At thermal equilibrium the reciprocal heat fluxes are balanced. The principle of detailed balance holds: the number of phonons is balanced at any momentum and energy. The phonons are considered to be quanta of acoustic vibrations of the lattice and are transmitted through a flat boundary in accordance

with the theory of acoustics. In the process, diffraction occurs as described by Snell's law (i.e., the momentum component parallel to the surface is conserved); the transmission probability is determined by the mismatch of the acoustic impedances of the media.

The amount of energy transmitted into each side is determined by the expression

$$\dot{Q} = \int_{\Omega} \varepsilon(p) \dot{n}(p, \tilde{T}) \alpha(p) d\Omega, \quad (3)$$

where ε is the phonon energy, p is the phonon momentum, $\dot{n} = v_z / \{1 - \exp[-\varepsilon(p)/k_B T]\}$ is the number of phonons with a given momentum that reach the boundary per unit time, $\alpha(p)$ is the probability of transmission through the interface (this probability must be calculated under certain assumptions about the scattering mechanism or it must be measured), and $d\Omega = dp^3 / (2\pi\hbar)^3$ is an element of the phase volume. The tilde refers to phonons moving toward the boundary; \tilde{T} is the equilibrium temperature and $\tilde{\Omega}$ is the part of the phonon phase space where the phonon velocity component v_z has a definite sign. Thus, in choosing the integration region, it is the group velocity $v_z = \partial\varepsilon/\partial p_z$ and not the z -component of the phonon momentum that is important.

Equation (3) is applicable if there exists an equilibrium temperature \tilde{T} of phonons moving toward the boundary. An important special case satisfying this condition is an interface between two media which are strongly mismatched acoustically, when the angle-averaged transmission coefficient is small.

In thermal equilibrium, of course,

$$\dot{Q}_1 = \dot{Q}_2, \quad (4)$$

but if the media in contact have different temperatures, the heat flux through the boundary will be

$$\dot{Q} = \dot{Q}_1(\tilde{T}_1) - \dot{Q}_2(\tilde{T}_2) \quad (5)$$

or, using Eq. (4),

$$\dot{Q} = \dot{Q}_1(\tilde{T}_1) - \dot{Q}_1(\tilde{T}_2), \quad (6)$$

$$h_K = \frac{d\dot{Q}}{d(\Delta T)} = \frac{d\dot{Q}_1}{dT_1}. \quad (7)$$

The possibility of taking into consideration only the transmission of acoustic phonons from one medium into another, as follows from Eq. (7), which takes into account the principle of detailed equilibrium, is important. It is this important feature that is the basis of the present work. We investigated only the transmission of phonons from liquid ^4He into a copper single crystal, and we assumed that the reverse process of phonon emission into helium corresponds precisely to the first process.

1.3. Dissipative acoustic model

The acoustic mismatch model identifies the probability of phonon transmission through an interface with the acoustic energy transmission coefficient α , calculated on the basis of the acoustic theory. In the nondissipative case, the transmission coefficient from liquid helium into a solid is very small because the media in contact are acoustically strongly mismatched: $\alpha \sim 4Z_{\text{He}}/Z_s = 4\rho_{\text{He}}c_{\text{He}}/\rho_s c_s \sim 10^{-3}$ (here ρ is the density, c is the sound speed, Z is the surface impedance, and the indices He and s refer to liquid helium and the solid, respectively), and vanishes outside a critical cone of angles of incidence, the size of the cone being determined by the critical angle of total internal reflection. The critical angle ϑ_i is also small, because the speed of the slowest transverse waves in a solid is significantly higher than the sound speed in liquid helium: $\vartheta_i \approx c_{\text{He}}/c_t \sim 0.1$. Here and below, subscripts l , t , RW, and PSW refer, respectively, to longitudinal, transverse, purely surface Rayleigh, and pseudosurface waves. The average probability of transmission of a phonon from liquid helium into a solid for arbitrary direction of incidence can be estimated as $Z_{\text{He}}\vartheta_{\text{He}}^2/Z_s\vartheta_s^2 \sim 10^{-5}$; it is because this probability is low that the thermal boundary resistance is significant.

The acoustic transmission coefficient is, however, sensitive to the presence or absence of dissipation in the medium. The main effect of dissipative processes for low phonon absorption is associated with the appearance of an additional energy-exchange channel—resonant modes on the surface.

A surface wave is completely localized near the boundary. Therefore, when the resonance conditions are satisfied, the wave can be acoustically well-coupled to a volume wave in the less dense medium. A phonon incident on the interface from the less dense medium at some angle $\vartheta_{\text{RW}} \approx c_{\text{He}}/c_{\text{RW}}$ excites a high-amplitude surface wave. In the absence of dissipation, localization precludes the propagation of the energy of the surface wave into the acoustically denser medium, so that the surface wave cannot participate in heat exchange. Even with weak dissipation ($p \gg 3 \cdot 10^{-4}$), however, the significant energy stored in the surface wave is dissipated directly near the surface, and is removed either by phonons scattered in bulk or by conduction electrons, depending on the specific dissipation mechanism.

This anomalous transmission of acoustic energy at an angle of incidence exceeding the critical Rayleigh angle was first studied by Andreev.^{3,4} He showed that the transmission coefficient at resonance reaches unity (compared to $\sim 10^{-3}$ for the continuous spectrum),³ and the efficiency of the new heat-conduction channel formed in this case is of the same order of magnitude as for heat transfer in which only volume modes participate, and it therefore reduces the observed Kapitza resistance by approximately a factor of 2.⁴

Resonant Rayleigh transmission of sound with amplitude ~ 0.01 was first observed experimentally by Zinov'eva.^{5,6} The experimental results presented in the present paper show that it is possible to observe resonant transmission of phonons with an amplitude of 0.1, which is an order of magnitude higher than observed in previously published works.

As the absorption coefficient p increases to values of the order of unity, an even larger increase in the Kapitza conductance is observed. This is due to the fact that when there is a large uncertainty in the phonon momentum due to the high absorption, the condition restricting the phonon emission angles to a critical cone is violated and the phonons escape into liquid ^4He at large angles. Then the integration region in Eq. (3), equal in the absence of dissipation approximately to the squared critical angle of incidence, becomes much larger. Such large values of the phonon absorption can be easily achieved near a surface, where the crystal lattice of the material is, as a rule, highly defective.

1.4. Experiments on phonon scattering at the interface between two media

The shortcomings of existing theories of the Kapitza resistance at all temperatures make direct experimental measurements of phonon transmission through the interface between two media of great interest. Both the angular spectra $\alpha(\vartheta)$ and the frequency spectra $\alpha(f)$ of the phonon transmission/reflection coefficient are investigated.

Angular spectra. In Ref. 7, Wyatt *et al.* present the results of their measurements of the angular spectra of scattering of thermal phonons at the interface between NaF and liquid ^4He . In their scheme phonons are emitted by the flat surface of a NaF single crystal, pass through a layer of liquid helium, and strike a thin-film bolometer, where they produce the recorded increase in the temperature of the bolometer. The angular distribution of the emitted energy can be observed by rotating the NaF sample.

The spectrum measured by Wyatt *et al.*⁷ consists of a peak of width $\sim 20^\circ$ at the center and a broad tail, decaying as the cosine of the phonon emission angle ($\cos \vartheta$). The size of the peak corresponds to the size of the critical cone, so that the central peak most likely corresponds to the processes described by the AMM. Unfortunately, the peak does not contain any features, and the absolute amplitude of the peak is unknown. For this reason it is impossible to relate the central peak to a specific scattering process with any certainty.

The wide tail of the spectrum is probably associated with the fact that some phonons incident on the boundary are diffusely scattered. First, this is indicated by the nature of the decay of the tail with increasing angle ϑ from the normal direction— $\alpha(\vartheta) \propto \cos \vartheta$, corresponding precisely to completely diffuse scattering (Lambert's law). Second, direct measurements show that phonons emerging at large angles have lower energies than phonons emerging within the critical cone. Further investigations Wyatt *et al.* showed that when the film bolometer, whose susceptibility does not depend on the phonon energy, is replaced by a tunnel junction that is sensitive only to excitations with frequencies above 90 GHz, the observed intensity in the tail becomes less than that of the central peak.⁸ Thus the heat-transfer channel responsible for the presence of the wide tail in the spectrum is probably inelastic and therefore diffuse. We note that the wide tail of the spectrum makes an approximately 1.5 orders of magnitude larger contribution to the Kapitsa resistance than the central peak, which supposedly corresponds to AMM transmission (thanks to the very large region of the phase space with approximately the same amplitude). The latter fact explains very well the reason for the discrepancy of this order of magnitude between the experimental values of the Kapitsa resistance and the predictions of the AMM.

It would be desirable, however, to resolve certain features of the transmission spectrum inside the critical cone. The AMM predicts several transmission zeros and resonance peaks in this section of the spectrum. The main reason for the low angular resolution in Ref. 7 is that incoherent thermal phonons were employed. The angular resolution is then determined by the angular dimensions of the emitter and the detector. The experimental situation is such that the resolution can be increased only by decreasing the amplitude of the useful signal (either the distance between the emitter and the detector must be increased or their dimensions must be decreased). The second possible reason is that significant scattering of phonons occurs at the comparatively high temperatures of 1–2 K employed in Ref. 7.

These deficiencies were eliminated by Zinov'eva,^{5,6} who investigated both the angular and frequency transmission spectra of low-frequency phonons passing from liquid ⁴He into gold and tungsten at ultralow temperatures of 0.06–0.4 K and at frequencies 10–30 MHz. Coherent phonons were generated by an ultrasonic quartz transducer. The experimentally measured spectra contain well-resolved features predicted by the theory—Rayleigh peaks along the edges. In general, it must be expected that at low temperatures and phonon energies the scattering processes at the interface are described well by the AMM, so that further investigations in this region are of definite interest. The work described in the present paper is, from the experimental standpoint, a further elaboration of the method developed by Zinov'eva and described in Refs. 5 and 6.

The very high absolute angular resolution required in order to observe features of the spectrum inside the critical cone is necessitated by the small dimensions of the cone (3°–10°). Hence it follows naturally that the low angular

resolution can be compensated by performing measurements on the solid-body side and not on the liquid-helium side. In this case the critical cone is a full hemisphere, and for the same absolute angular resolution it is possible to achieve $c_s/c_{\text{He}} \sim 10\text{--}30$ times higher relative resolution in accordance with Snell's law of refraction. This idea was recently employed by Kinder.⁹

Our results indicate that the acoustic mismatch model is valid for the case investigated (carefully prepared surface at a temperature of 1 K). Indeed, resonances were observed in good agreement with the theory. It should be noted, however, that volume focusing makes it very difficult to interpret the results. Moreover, this measurement scheme makes it impossible to observe resonant energy transmission associated with the existence of purely surface Rayleigh modes at the interface: there is no volume mode that corresponds to the surface Rayleigh modes.

The silicon single crystal investigated in Ref. 9 has strong acoustic anisotropy, and this justifies measuring the two-dimensional transmission pattern. It is by comparing the general form of the two-dimensional theoretical and experimental spectra that the authors draw conclusions about the character of phonon scattering processes at the interface. In the present paper, we also present results of measurements of the phonon transmission coefficient for all possible directions. Taken together, these results show reliably that the AMM is in good agreement with the experimental data.

Frequency spectra. The frequency spectra of boundary scattering have been measured in a large number of works (see the reviews Refs. 10 and 11 and the references cited there) over a wide range of frequencies (up to thermal and higher).

Eisenmenger *et al.*¹² measured the frequency dependence of the internal reflection coefficient for monochromatic phonons in a tin single crystal. A beam of phonons with frequencies of 70–200 GHz, which was produced with a Josephson junction, was reflected from the Sn–⁴He interface and recorded with the help of a bolometer. At frequencies above 85 GHz the reflection coefficient decreases substantially. This reduction is probably due to diffuse scattering, which predominates at high frequencies. The frequency $f=85$ GHz corresponds to the temperature $T=2\pi\hbar f/k_B \simeq 4$ K (it must be borne in mind that the maximum phonon energy occurs at three times this frequency $f_{\text{max}}=3 k_B T/2\pi\hbar$, and that the influence of diffuse scattering on the Kapitsa resistance becomes appreciable at 1.5 K).

Since in Ref. 12 the results are normalized, it remains unclear how large the phonon transmission is at low frequencies. The method employed (reflection) is too inaccurate in order to judge the absolute transmission at the beginning of the spectrum, because this part of the spectrum is very small. In order to measure the transmission coefficient α , which approximately 0.005 according to the AMM, it is necessary to know the reflection coefficient to an accuracy of $\alpha/(1-\alpha) \simeq \alpha \sim 0.005$, the error in this case being 50%. This difficulty is related directly to the existence of the boundary resistance: little is transmitted but

much is reflected. Therefore, direct measurements of transmission are preferable. This is the scheme that we employed to obtain the results presented in the present paper.

The sensitivity can also be increased by using an experimental scheme in which multiple reflections of phonons from the faces of the crystal are employed to increase the total transmission. In this case, naturally, as a result of n reflections, the observed reflection coefficient increases by a factor of n . Pohl and Olson employed this idea to measure the transmission of equilibrium thermal phonons from a silicon single crystal into liquid helium.¹³ They measured the effective thermal conductivity of a thin cylindrical silicon plate in the radial direction. Since phonons propagate ballistically in silicon, the only scattering mechanism limiting the thermal conductivity is scattering at the interface. They studied thermal conductivity in two cases: a sample in vacuum and in liquid helium. The difference between the thermal conductivities was attributed to phonon scattering in helium. Due to the thinness of the plate, numerous reflections from the boundary occurred and the sensitivity of the method was increased significantly.

Pohl and Olsen's work¹³ has the advantages¹⁾ that equilibrium thermal phonons were used for the measurements and that the absolute transmission was determined without normalizing the results (in contrast to all other work discussed here).

All experimental results cited above, taken as a whole, show that at temperatures of the phonon gas below 0.5 K, the transmission probability agrees with the predictions of the AMM; at higher temperatures the transmission coefficient starts to increase rapidly, in accordance with the higher contribution of diffuse scattering.

2. THEORY OF TRANSMISSION OF ULTRASONIC ENERGY THROUGH THE INTERFACE BETWEEN TWO MEDIA

2.1. General scheme of the transmission coefficient coefficients

Our general method for calculating the acoustic-energy transmission coefficient is as follows (see, for example, Ref. 14):

The equation of motion (wave equation) of an unbounded medium is written out and solved.

The boundary conditions for a bounded medium are written out.

The solutions obtained in the first step are used to construct a linear combination satisfying the boundary conditions.

This separation of the problem into steps, though arbitrary, is not artificial. The problem was solved on a computer in this order, and each step was implemented as an independent subprogram. Calculations according to this scheme can be easily monitored, and make it possible to obtain intermediate results. All three steps can in principle be combined into a single large algebraic equation (i.e., the transmission coefficient is the root of some polynomial of very high degree, constructed from the elastic moduli and densities of the media in contact), but this equation can hardly be solved with existing computational resources.

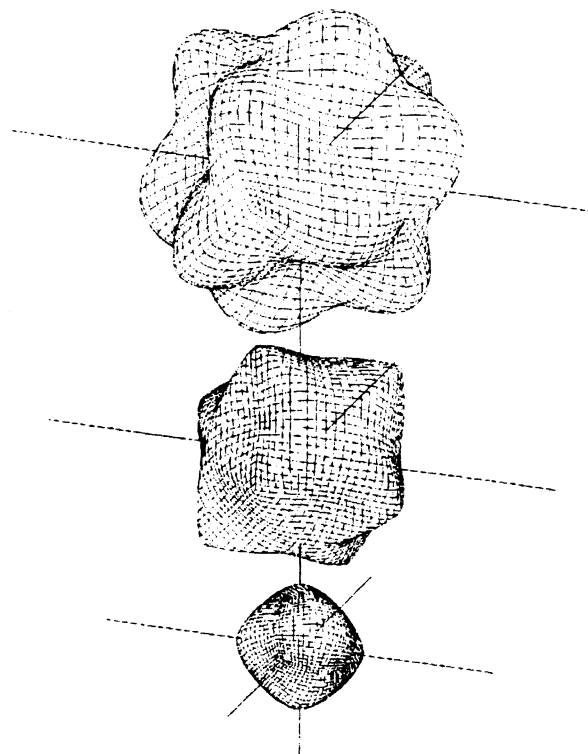


FIG. 1. Isofrequency surfaces in copper in acoustic wave-vector space. The surfaces corresponding to the longitudinally polarized mode (top) and fast and slow transverse modes (center and bottom) are displayed. The surfaces have a common center, but they are separated in the figure along the vertical coordinate. The crystallographic axes $\{100\}$ are shown.

2.2. Acoustic waves in an anisotropic medium

Let an acoustic wave with frequency ω , wave vector k_i , and polarization X_j (i.e., $u_j = X_j \exp[ik_j x_j - \omega t]$) propagate in a medium with elasticity λ and density ρ . We write the wave equation in the form

$$(k_i k_j \lambda_{ijkl} - \rho \omega^2 \delta_{jk}) X_j = 0. \quad (8)$$

Equation (8) yields a relationship between ω , k_i , and X_j . Since the right-hand side is zero, nontrivial solutions for X_j can exist only if

$$\det(k_i k_j \lambda_{ijkl} - \rho \omega^2 \delta_{jk}) = 0. \quad (9)$$

The latter relation yields the acoustic dispersion of the medium $\omega = \omega(k_j)$, or it can be regarded as an equation for the absolute magnitude of the wave vector as a function of the frequency ω and direction n_j in the crystal: $k = k(\omega, n_j)$. In this form it is a bicubic polynomial in k and, therefore, it has three pairs of roots $k^{(m)}(\omega, n_j)$, corresponding to one longitudinal and two transverse modes.

Three isofrequency (isoenergy) surfaces of copper, calculated by the authors, are displayed in Fig. 1 in wave-vector space. All three surfaces have a common center at the point $k_i = 0$ and lie inside one another. In the graphical construction, however, they are displaced along the ordinate so that they can be examined separately. The surface of longitudinal phonons is displayed at the top; this is the smallest surface, because of the fact that the longitudinal

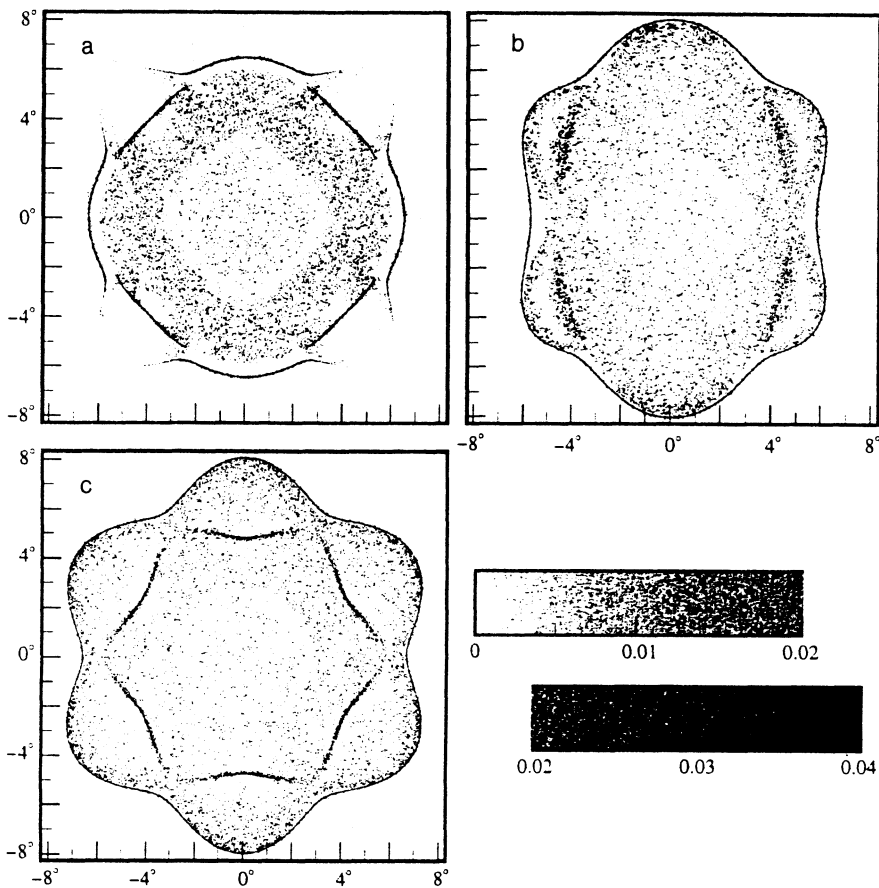


FIG. 2. The results of theoretical calculations of the transmission of acoustic energy through the interface of liquid ${}^4\text{He}$ and a copper single crystal cut in the planes (001) (a), (011) (b), and (111) (c). Two components of the angle of incidence of ultrasound on the interface are plotted along the axes; higher transmission coefficients correspond to darker grays in the figure in accordance with the gray scale in the bottom right-hand corner. The calculation was performed for absorption $p=5 \cdot 10^{-4}$. The straight lines crossing the spectrum in Fig. 2a show the scan directions along which the experimental measurements were made (see Fig. 7).

wave propagates with the highest speed. The surface of the fast transverse mode is displayed at the center and the surface of the slow transverse mode is displayed at the bottom.

Due to the significant acoustic anisotropy of copper, the surface corresponding to the slowest mode (this is the largest surface and is displayed at the bottom in Fig. 1), is nonconvex; it is this feature that is responsible for the appearance of a pseudosurface mode and the transition from the standard to the generalized surface waves.¹⁵ In the isotropic case, all three surfaces would naturally be spherical, and the surfaces corresponding to the transverse modes would have equal diameters (complete degeneracy).

The following circumstance is also interesting. It is in principle impossible to separate the two surfaces corresponding to the transverse modes. In reality, they comprise a single two-sheeted surface. This is a topological property of the sphere: if directions of degeneracy did not exist, then each surface could be tagged according to its transverse polarization. It is well known, however, that this is impossible to do (see, for example, Ref. 16). Therefore, there always exist directions (at least two) in which the transverse wave is doubly degenerate. For a cubic copper crystal such directions are $\{100\}$, where the surfaces are tangent to one another, and $\{111\}$, where one transforms into another, forming a conical funnel. Conical points in the directions $\{111\}$ can be clearly seen in Fig. 1 (these are the sharp corners of a "cube" and pointed depressions on a

"potato"); when the surface is constructed it is artificially cut into two sheets at these locations.

2.3. The interface Orientation of the boundary, choice of coordinate axes

We now assume that there exists a flat interface. To simplify the equations, it is necessary to choose a coordinate system whose axes differ from the crystallographic axes, but which is tied to the boundaries of the media. Specifically, the z axis must be perpendicular to a boundary, which then satisfies the equation $z=0$ (liquid helium on top). This condition is a stringent one for the given sample, since the crystallographic direction of the sample surface is fixed. The choice of the other two axes is arbitrary, however.

In studying the transmission of ultrasound for all possible directions (which is our objective here), it is convenient to fix the x' and y' axes and the direction of incidence by the two components of the wave vector lying in the plane of the interface:

$$k'_x c = \omega \sin \vartheta \cos \varphi; \quad k'_y c = \omega \sin \vartheta \sin \varphi. \quad (10)$$

Here ϑ is the angle of incidence of the ultrasound and φ is the azimuthal direction with respect to a fixed coordinate system. This scheme was adopted to construct the two-dimensional transmission spectra shown in Fig. 2.

The coordinate system (unprimed hereafter) whose x axis was rotated into the sagittal plane was actually employed in the calculations. In this case

$$k_x c = \omega \sin \vartheta, \quad k_y = 0, \quad k_z c = \omega \cos \vartheta. \quad (11)$$

In this coordinate system only the single quantity k_x need be given, and for this reason the equations are simplest in this system. The procedure for taking anisotropy into account in this approach reduces to first rotating the elasticity tensor, defined in the standard fashion, to the new axes.

Boundary conditions. The boundary conditions at the interface reduce to conservation of the tangential component of the wave vector (Snell's law) and the continuity equations. Assuming that an acoustic wave with wave vector k_i^{He} is incident from the liquid ^4He side, we obtain the reflected and transmitted waves whose vectors and frequencies satisfy the conditions

$$k_x = k_x^{\text{He}}, \quad k_y = k_y^{\text{He}}, \quad \omega = \omega^{\text{He}}, \quad (12)$$

where the z component of the reflected wave $k_{z\text{refl}}^{\text{He}}$ is the negative of the z component of the incident wave (specular reflection); the z components of the waves transmitted into the crystal are determined from the dispersion equation (9). The latter equation is a polynomial of degree six in k_z , and it must therefore have six different roots (possibly imaginary). From the six waves with a suitable tangential component of the wave vector it is necessary to choose three waves corresponding to the physical requirement of causality. If the roots are real, this choice is made according to the group velocity (downward), and if the root is complex, it is made according to the imaginary part (amplitude decreasing into the solid).

The continuity conditions reduce to equality of the normal displacement and stress and absence of tangential stresses σ , i.e., to a linear system of equations from which the amplitude of the reflected wave can be found. (We neglect the viscosity of the liquid, but we take into account sound absorption due to the viscosity of the solid.) By comparing it to the amplitude of the incident wave, we can obtain the reflection coefficient; subtracting the reflection coefficient from unity we obtain the transmission coefficient $\alpha(\vartheta, \varphi)$. The angle φ gives the rotation angle of the sagittal plane in the boundary plane of the sample.

2.4. Computational results for the transmission coefficient of the liquid-helium-copper interface

We employed the computational scheme described above to investigate theoretically the two-dimensional pattern of acoustic energy transmission through the interface between two media. The computer program developed for this purpose makes it possible to calculate the coefficient of transmission into a crystal with arbitrary symmetry through an arbitrarily oriented boundary. The program's efficiency can be expressed in terms of the number of operations required to obtain a single value of $\alpha(\vartheta, \varphi)$. This efficiency is $1.5 \cdot 10^4$ flops/point.²⁾

Figure 2 displays the computational results for sound transmission through different faces of a copper single crystal. The gray-scale density indicates the magnitude of

the transmission coefficient as a function of the two angular components of the incidence direction of sound on the plane (darker gray corresponds to higher transmission). The more familiar one-dimensional spectra for certain directions in a plane close to the (001) plane of copper are displayed below in Fig. 7 (dotted line).

Examination of the two-dimensional spectra shows that the features observed in an isotropic body are also present in the anisotropic case. A region of transmission of longitudinal sound is observed at the center at angles close to normal incidence. Due to the anisotropy of the medium, the region is not circular, and its shape corresponds to the projection of the isofrequency surface of longitudinal waves (see Fig. 1) on each of the chosen planes; it is separated from the region of transverse waves by zero transmission.

As in the case of an isotropic body, transmission in the region of transverse waves is higher than in the region of longitudinal waves, but here there are additional features associated with the excitation of two transverse modes rather than one, each of which gives rise to a feature at its critical angle of incidence.

Figure 2 also contains sharp peaks in the transcritical region. They are visible as narrow black bands bordering the continuous spectrum. They correspond to resonant sound transmission accompanying the excitation of a Rayleigh surface wave. Outside the critical cone the transmission coefficient drops rapidly to zero.

The main difference from the isotropic case is that secondary resonance peaks, corresponding to pseudosurface waves, appear in the region of the continuous spectrum. They can be seen in the (001) plane near the {110} directions. The transmission intensity associated with a purely surface Rayleigh mode vanishes in the same directions. This is the (001) plane of copper, and we chose this plane for experimental investigation.

2.5. Surface waves in the anisotropic case

The existence of a surface wave in the anisotropic case for arbitrary direction and arbitrary plane is by no means obvious. In 1955, for example, Stonely¹⁷ incorrectly discarded an entire class of solutions corresponding to generalized surface waves, and thus arrived at the conclusion that surface waves do not exist in the (001) plane for an entire class of cubic crystals. Later it was shown, however, that a solution which is completely localized near the surface does exist in the arbitrary case.¹⁸

The main difficulty is that the condition of zero surface impedance is very stringent in the following sense. In solving the wave equation (8) with a definite wave vector k_x , we obtain six suitable roots k_z , which, generally speaking, are complex. The surface impedance $Z(k_x)$ is therefore also a complex function of the real variable k_x . Thus, the impedance trajectory representing a one-directional manifold in the two-dimensional complex plane may not pass through a definite point $0+i0$ on it. It is important to remember, however, that if the parallel component of the wave vector k_x is greater than the critical component, then the impedance must be purely imaginary for total internal

reflection to be observed at the corresponding angle of incidence of sound from the liquid. Therefore, in the supercritical region the condition of existence of a surface wave reduces to passage of a one-dimensional trajectory on a one-dimensional straight line through a point, i.e., it reduces to an inequality. We note that the conclusion that a surface wave exists can be drawn by examining the problem (not directly related to the conclusion) of the transmission of an acoustic wave from a liquid into a crystal.

We now examine a surface wave propagating near the [110] direction in the (001) plane of copper. It is well known that the velocity of a surface wave is somewhat lower than the velocity of the slowest volume wave propagating in this direction.³⁾ In an isotropic body, their ratio $\xi = c_{RW}/c_t$ lies in the range $0.874 < \xi < 0.955$ (Ref. 19, p. 137). It must therefore be expected that the surface mode will lie immediately beyond the limit of the continuous spectrum. However, this will not be so for a wave propagating precisely in the [110] direction. The problem is that the slowest volume wave, which lies in the sagittal plane (110), is polarized in the plane of the interface, and its impedance therefore vanishes at the point corresponding to the limit of the continuous spectrum. As the azimuthal angle approaches 45° , the Rayleigh angle approaches the critical angle of transmission of the transverse mode, and it equals the critical angle exactly in the [011] direction. Such a degenerate solution is not a true surface wave, since its transverse wave vector k_z is real and there is no localization. Near the [011] direction, the imaginary part of the transverse wave vector of the Rayleigh wave is very small and the wave penetrates deep into the crystal (the amplitude of the wave is oscillatory). Such behavior of the solution is characteristic of strongly anisotropic media and appears if the isofrequency surface is nonconvex.¹⁵ In the isotropic case the amplitude of the wave decays exponentially into the crystal without oscillating. The oscillatory solution is customarily termed a generalized surface wave.

The fact that the Rayleigh wave approaches the continuous spectrum near the azimuthal direction 45° means that in these directions $1 - \xi$ approaches zero. This has the following obvious consequences as the azimuthal angle approaches 45° :

1) The acoustic coupling of the surface wave to the liquid, as determined by the radiative damping p^{RW-He} , can be arbitrarily small. Since the critical absorption p_c , at which the amplitude of energy transmission reaches unity, equals the acoustic coupling between a surface wave and the surface $p^{RW-He} = p_c$, the fact that the critical absorption drops to zero results in the fact that anomalous (~ 1) sound transmission into the solid takes place with very low absorption. In particular, in contrast to the isotropic case analyzed in Ref. 3, the scattering of the wave by conduction electrons can give rise to anomalous transmission, even when the electron mean free path is much shorter than the wavelength of the sound. The latter assertion is illustrated in Fig. 3.

2) The peak becomes arbitrarily narrow. The small width of the peak corresponds to weak acoustic coupling between the surface wave and the liquid, and a well-defined

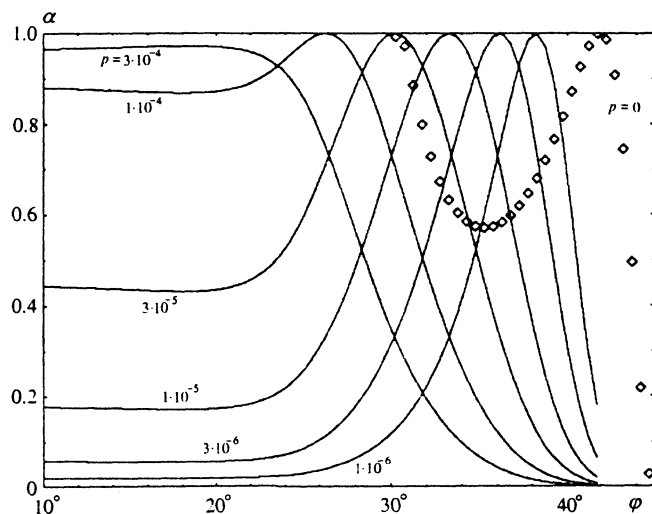


FIG. 3. Amplitude of resonant transmission of acoustic energy as a function of direction in the (001) surface for different values of the absorption p . For very small values of the absorption, anomalously high transmission is observed near the [110] direction ($\varphi = 45^\circ$); in addition, for arbitrarily small values of p there exists a direction in which the transmission amplitude reaches unity (this follows from the topology of the impedance trajectories). The resonant peak becomes arbitrarily narrow as the 45° direction is approached. The solid curves represent a purely surface wave. \diamond —amplitude of sound transmission with excitation of a pseudosurface wave in the nondissipative case $p=0$. The amplitude reaches unity at an angle of 42° , when the emission of a pseudosurface wave p^{PSW-S} equals the emission into the liquid p^{PSW-He} . At an angle of 30° , the transmission amplitude once again becomes unity, and the pseudosurface wave transforms into a volume wave with zero surface impedance. The pseudosurface branch vanishes at azimuthal angles less than 30° .

wave vector of the surface wave. We note that we are employing a model that neglects viscous stress in the liquid; over the range of angles considered, however, this assumption sooner or later becomes untenable, since this channel for energy exchange starts to dominate over the elastic channel.

3) The narrowing of the peak is simultaneously accompanied by a decrease, in the same ratio, of the magnitude of the integrated transmission I_{RW} , which vanishes at the azimuthal angle 45° . The behavior of the integrated transmission as a function of the azimuth of the sagittal plane is displayed in Fig. 4.

2.6. Pseudosurface waves

The surface wave in the [011] direction still exists. Indeed, since the slow transverse wave in the (110) plane is polarized "incorrectly," it has no effect at all on the surface impedance. The situation is exactly analogous to that of an isotropic body, for which the system of boundary conditions of the solid decomposes into two independent conditions: the mode polarized in the plane of the boundary is responsible for the vanishing of the stresses σ_{yz} . The two other conditions for σ_{xz} and σ_{zz} are satisfied by the longitudinal mode and the transverse mode polarized in the sagittal plane.

Now, if the incorrectly polarized mode is dropped, then we find another solution with zero impedance. This

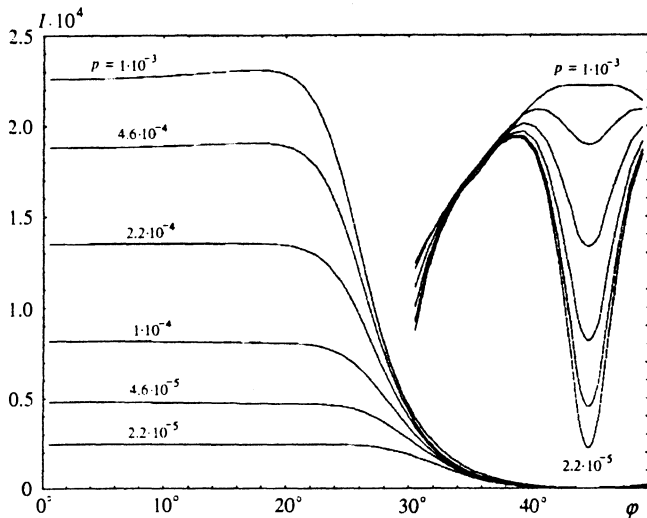


FIG. 4. The integral $I = \int \alpha(\vartheta) d\vartheta$ of the resonant energy transmission as a function of azimuthal direction in the (001) surface for different values of the absorption. The integrated transmission for a purely surface wave (curves on the left) vanishes in the direction 45° . The integrated transmission of the pseudosurface wave (curves on the right) in the directions 30 – 42° does not depend on the dissipation, since the emission of radiation into the solid body is stronger than emission into the liquid. In the opposite case, occurring in the azimuthal directions 42 – 48° , I_{PSW} depends on the dissipation if the dissipation is greater than the emission into the crystal and less than the emission into the liquid: $p^{\text{PSW-s}} < p < p^{\text{PSW-He}}$. In the direction 45° , the pseudosurface wave degenerates into a purely surface wave.

solution lies in the continuous spectrum and has a velocity somewhat lower than that of the slowest of the remaining modes. This solution will be a true surface wave, and even though it lies in the continuous spectrum it is nonetheless completely localized near the surface, since the only volume wave into which the surface wave could emit energy with conservation of momentum is polarized orthogonally to its characteristic polarization vector.⁴⁾

Near the [110] direction, the solution similar to the one considered above will no longer be a purely surface mode, since in nearby sagittal planes the polarization of the slowest transverse wave is no longer orthogonal to the given solution, and it will therefore interact with the solution, carrying away the energy of the surface wave into the volume of the solid. It can be expected, however, that orthogonality does not break down strongly near 45° , and losses due to radiation into the solid will be small compared to the energy localized near the surface. By analogy with the previously considered surface mode at the interface between a crystal and liquid helium, the radiative losses can be taken into account by introducing the radiative damping coefficient $p^{\text{PSW-s}}$ of the wave under consideration. The total damping of the surface wave now consists of the dissipation p and losses due to radiation into the liquid ($p^{\text{PSW-He}}$) and into the solid ($p^{\text{PSW-s}}$). Such waves, though they are not completely localized near the surface, are coupled quite weakly to the volume modes, and they are customarily termed pseudosurface waves. The transition from a purely surface wave propagating in the 45° direction to pseudosurface waves is illustrated in Fig. 5.

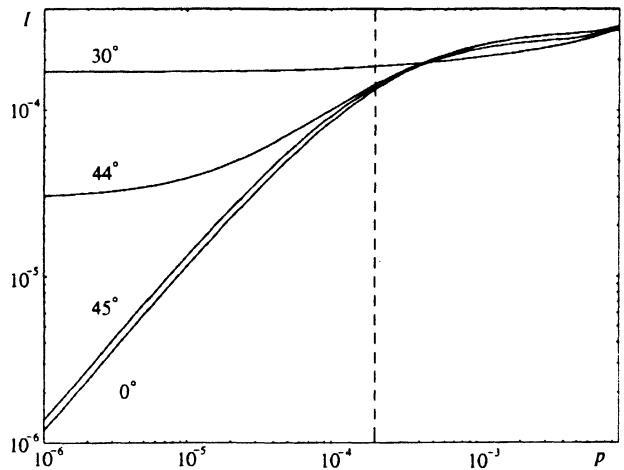


FIG. 5. The integrated weight I of resonant energy transmission as a function of absorption p for different types of surface modes on the interface between liquid ^4He and Cu versus the absorption p . The curves for four azimuthal directions in the (001) plane of copper are presented: 0 , 30 , 44 , and 45° from the [100] axis. In the directions 0 and 45° —purely surface modes, 30° —purely pseudosurface mode, and 44° —intermediate case. Dashed line—natural radiative damping of the surface mode $p^{\text{RW-He}} \sim (1 - \xi) Z_{\text{He}}/Z_{\text{Cu}}$, associated with emission into the liquid. The differences in behavior clearly vanish for $p > p^{\text{RW-He}}$.

3. EXPERIMENTAL PROCEDURE

3.1. Method for measuring the phonon transmission coefficient of the interface

The measurement method is based on measuring the heating of the sample relative to the liquid helium by the acoustic energy transmitted into the sample.

Phonons with energy flux χ_i incident on the surface of the sample are scattered. As a result, some phonons are reflected backwards, some are transmitted into the sample, and some are absorbed at the surface:

$$\chi_z + \chi_z^{\text{refl}} + \chi_z^{\text{trans}} + \chi_z^{\text{abs}} = 0. \quad (13)$$

The last two terms give the total energy \dot{q} transmitted through unit area of the sample surface, where the energy is dissipated and converted into heat. Actually, the term χ_z^{trans} describes the flux of coherent phonons, and the hypothesis that the transmitted energy is totally thermalized must therefore be additionally checked. Specifically, the observed slow thermalization effect will be discussed in Sec. 4.4, when we discuss the measurement results. Thus

$$\dot{q} = \chi_z^{\text{trans}} + \chi_z^{\text{abs}}. \quad (14)$$

The quantity of interest to us, specifically, the acoustic-energy transmission coefficient α , is defined as

$$\alpha = \frac{\dot{q}}{\chi_z}. \quad (15)$$

None of the quantities in the definition (15) can be measured directly. The power flux χ_z per unit area is defined as the corresponding component of the power flux χ_i emitted by a quartz transducer for a given angle of incidence ϑ :

$$\chi_z = \chi \cos \vartheta. \quad (16)$$

The power of the quartz transducer can be calculated from the known voltage applied to its plates, or it can be measured directly. The cosine of the angle of incidence is essentially unity for the angles of incidence of interest to us: $\vartheta \sim 6^\circ = 0.1:1 - \cos \vartheta \simeq \vartheta^2/2 \sim 0.005$. In all of the following calculations, we therefore set $\cos \vartheta = 1$.

The energy transmitted into the sample heats the sample with respect to the liquid. All energy transmitted into the sample is removed through the boundary in the form of heat. The main obstacle to this process is the boundary resistance, and therefore the observed heating ΔT of the sample is related to the energy \dot{Q} transmitted into the sample as

$$\Delta T = \frac{S_{\text{exp}}}{S_{\text{sample}}} R_K \dot{q}. \quad (17)$$

Here S_{exp} is the area of the sample upon which the phonon flux is incident, S_{sample} is the total surface area of the sample through which the heat is removed, and R_K is the Kapitza resistance per unit area. By measuring the heating ΔT as a function of the angle of incidence ϑ and the parameters appearing in Eq. (17), we can calculate the heat flux \dot{q} and thus the transmission coefficient $\alpha(\vartheta)$.

3.2. Construction of the measuring cell

The measuring cell is described in Ref. 6. The measuring chamber has the form of an upside-down beaker 40 mm in diameter and 50 mm high. The bottom of the beaker is also the bottom of the dissolution vessel. The sample, secured in a rotating frame, and the quartz, mounted on a small platform, are inserted in the chamber.

The sample is secured in the rotating frame with the help of a holder, which holds the sample in a position that makes it possible to investigate a definite direction. The sample is clamped between two textolite rings. Thus the assembled sandwich rotates freely in a brass ring. The ring is screwed to the rotating frame through two openings, clamping the sample with the rings at a definite angle with respect to the direction of rotation. The textolite rings with the sample clamped between them can be turned by the required angle by slightly releasing the securing screws. The front ring also limits the region exposed to the ultrasound to a flat section on the surface of the sample, covering the rounded corners by approximately 0.5 mm.

Seven index marks, one every 15° , were put on the front textolite ring in order to check the angle of rotation. The rotation angle of the sample can be set to within $\sim 1/5$ of the distance between the marks, i.e., 3° , by aligning the moving marks with the stationary mark on the brass ring. The measurements were actually performed for directions making angles of 0, 10, 22, 29, 37, and 45° with the [100] axis of the sample.

Two germanium thermometers were glued with electrically conducting glue to the back face of the sample in order to measure the heating of the sample. A constantan wire with a resistance of 41Ω (at liquid-helium temperature), laid in the form of a spiral, was glued to the sample

with BF glue. The conducting glue ensures electric and thermal contact, simultaneously, between the sample and the thermometers; the sample itself serves as a common terminal for both thermometers and is electrically insulated from ground. The heater is used to determine the Kapitza resistance of the sample and to calibrate the power transmitted into the sample.

The flexible electric input leads of the thermometers and heater are made of superconducting wire and are laid in the form of a ring. At the same time, the material of the input has zero resistance and very low thermal conductivity; the latter property is very important because of the nature of the measurement method employed. A similar requirement of low thermal conductivity dictates the choice of textolite as the material for the clamping rings. The measurements show that at all temperatures employed, the leakage of heat through the armature does not exceed 1% of the total heat flowing to the sample.

3.3. Sample

The sample used for the measurements was cut from a copper single crystal by the electric spark method, and had a diameter of 10 mm and a thickness of 1.4 mm. It had a slightly ellipsoidal shape, since the (001) plane made an angle of 18° with the axis of the initial cylindrical single crystal. The sample was mechanically polished with diamond paste and then electrochemically polished in orthophosphoric acid by the method described in Ref. 20. A $10\text{-}\mu\text{m}$ thick layer of copper was removed by electrolytic polishing. This is several times greater than the grain size of the coarsest diamond paste employed for mechanical polishing. Therefore, the surface obtained was free of mechanical stresses.

The surface of the sample was examined for smoothness and the presence of scratches with a Linnik interference microscope. Most of the surface was smooth to within 100 nm. Fine 200–500 nm deep scratches were also present with a density of ~ 1 scratch/mm. The rounded region at the edge of the sample extends over a distance of $50 \mu\text{m}$. Thus it can be expected that at ultrasonic wavelengths of up to $1 \mu\text{m}$, which corresponds to a frequency of 50 MHz, scattering by local surface defects is small.

The large-scale structure of the surface of the sample was also studied. For this, an image of the surface of the sample was digitized with a step of $0.5 \times 0.5 \text{ mm}^2$ and the data were analyzed with a computer. The surface of the sample deviates from a flat plane by not more than $10 \mu\text{m}$.

4. EXPERIMENTAL RESULTS AND DISCUSSION

4.1. Objective of the experiments

The purpose of the experiments was to obtain the angular dependence of the coefficient of transmission of phonon energy from liquid ^4He into the copper single crystal. The data obtained were then compared to the predictions of the generalized acoustic theory in order to determine how well the theory describes the effects which actually occur. In setting up the experiments we had the following circumstances in mind.

● From our standpoint the most interesting question is how the heat transfer occurs at the interface. In order to answer this question it is necessary to obtain the transmission spectra for the highest possible frequencies and lowest possible temperatures. A temperature of 100 mK corresponds to a phonon frequency of 2 GHz. If it were possible to obtain experimental data at such high frequencies, then it would be possible not only to compare them to the acoustic theory but also to determine how well this theory describes heat transfer processes involving thermal phonons, i.e., it would be possible to obtain information about the microscopic characteristics of Kapitza conductance.

● It is important to obtain experimental curves for all possible azimuthal directions of incidence of the ultrasound. Since copper exhibits strong acoustic anisotropy, the transmission spectra must be substantially different for different azimuthal angles of incidence of ultrasound. Reliable information can be obtained by comparing the data on the anisotropy to the theory, since the azimuthal direction was measured beforehand, no calibration is required, and it is known with good accuracy: $\sim 3^\circ$.

● It is important to make use of the possibility of observing resonant transmission of ultrasound accompanied by the excitation of surface acoustic modes on the interface. The existence of resonances together with excitation of a pseudosurface wave would be reliable confirmation of the applicability of the generalized acoustic theory. Measurement of the parameters of the peaks appearing when a purely Rayleigh surface wave is excited would make it possible to determine the unknown absorption parameter ρ , which plays an important role in the theory.

4.2. Range of the measurements

All measurements were performed on the same sample, prepared from a copper single crystal cut in a plane close to the (001) basal plane. In order to prevent oxidation and contamination of the surface of the sample between measurements, the experimental cell was kept in an evacuated desiccator.

The sound transmission coefficient as a function of angle, $\alpha(\vartheta)$, was measured at temperatures 100–400 mK and frequencies 13–270 MHz (Fig. 6). The frequency–temperature interval is limited at high temperatures by the absorption of ultrasound in liquid helium, at high frequencies by the quality of the quartz emitter, and at low temperatures by the low cooling capacity of the diffusion refrigerator and the long relaxation times (exceeding 1 sec). It follows from the figure that the measurements were performed at all possible temperatures in the cell and at frequencies of ultrasonic phonons for which the present measurement method can be used.

The measurements were performed at all possible angles of incidence for the (001) plane of copper. Six series of measurements were performed. In each series, the sample was mounted in a definite azimuthal direction, $\varphi=0, 10, 22, 29, 37,$ and 45° (Fig. 2a).

Since the symmetry group of the crystal lattice of copper (fcc) contains one symmetry axis and eight symmetry planes perpendicular to the surface of the sample, informa-

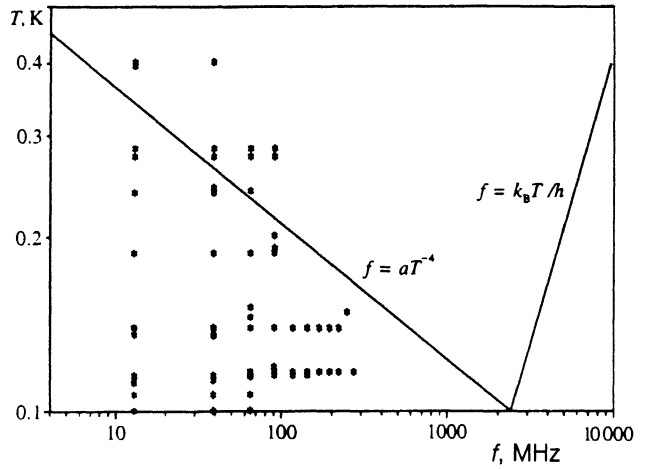


FIG. 6. Temperature and frequency ranges in which measurements of acoustic energy transmission into the copper single crystal were performed. A dot in the plot corresponds to each measurement. Above the straight line $f = aT^{-4}$, the phonon mean free path in ^4He becomes less than the quartz–sample separation (~ 5 mm). Measurements are difficult to perform at low temperatures because the time required to establish thermal equilibrium increases and the cooling capacity of the diffusion refrigerator decreases. The region of thermal phonons $f = k_B T / h$ is also shown; as follows from the figure, the maximum achievable frequencies are ten times lower than thermal phonon frequencies.

tion was also obtained simultaneously about another 15 symmetrically disposed trajectories. Thus, all possible azimuthal directions of incidence of ultrasound on the (001) plane of copper were investigated with a step of $\sim 4^\circ$.

4.3. General form of the experimental curves

The results of the measurements for different azimuthal directions are shown in Fig. 7 (solid lines). The dashed lines are the expected theoretical curves. As follows from the figures, the computational results agree very well with the measurements, repeating even subtle details. This is the first time that such agreement has ever been achieved.

Supercritical region. According to theory, heating of the sample by the incident ultrasound is observed only inside the critical cone. The range of allowed angles in copper is $-7^\circ < \vartheta < 7^\circ$. A sharp boundary is observed between the regions of energy transmission and total internal reflection. Since the transmission coefficient in the supercritical region decreases according to a power law

$$\alpha(\vartheta) \sim \kappa(\vartheta - \vartheta_{RW})^{-2}, \quad (18)$$

it is impossible to give the characteristic angular scale on which the transmission coefficient $\alpha(\vartheta)$ vanishes. Equation (18) contains a parameter κ with the dimensions [transmission units \cdot angle 2], and does not contain a parameter with the dimensions of angle. It can nonetheless be asserted that the decrease is in good agreement with theory, and the transmission coefficient decreases from $5 \cdot 10^{-3}$ (the transmission in the region of the continuous spectrum) to the noise level within an angular interval $\sim 0.5^\circ$. It is of interest to compare this result to Wyatt's result in Ref. 7, where the transition region occupies not less than several angular de-

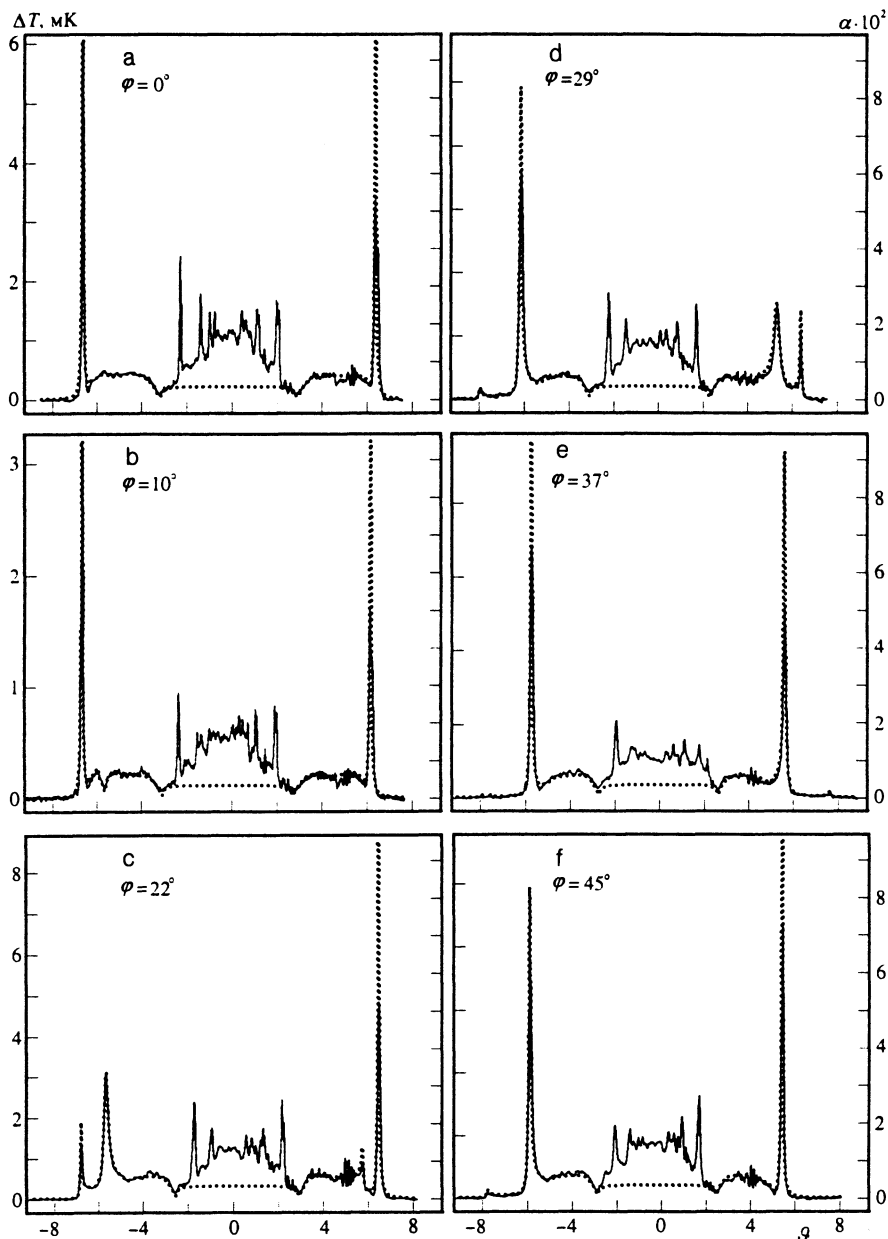


FIG. 7. Experimental spectra of phonon transmission into a copper single crystal. The spectra were measured along different azimuthal directions $\varphi=0, 10, 22, 29, 37,$ and 45° (the scan trajectories are shown in Fig. 2a); the temperature $T=140$ mK and the frequency $f=38.89$ MHz. The dotted curves were computed.

degrees. Moreover, Wyatt's phonon emission spectrum contains a wide tail, which decays as $\cos \vartheta$ and has an amplitude of the order of the signal amplitude within the critical cone.

The angular distribution of ultrasound transmission in tungsten published by Zinov'eva⁶ contains a tail extending into the supercritical region to a distance of about $1.5-2^\circ$.

Therefore, the results presented in this work indicate that the boundary of the critical cone may be five to ten times sharper than previously observed.

Resonant modes. Peaks corresponding to the excitation of resonant modes on the interface are well resolved in all spectra obtained. Both pseudosurface and purely surface Rayleigh waves are observed. They are all excited at angles of incidence that accurately correspond to the theoretically computed angles, and they contain parameters (width, height, and total weight) that are in reasonable agreement with theory.

In two of the six sagittal planes investigated—specifically, in planes making angles of 0 and 10° with the (010) plane of the crystal—only peaks corresponding to a purely surface Rayleigh wave were observed (Figs. 7a and 7b). The records obtained for all other sagittal planes (Fig. 7c–f) contain both types of features. This result is in accurate agreement with the theory of surface waves in anisotropic media¹⁴ and our calculations (see Fig. 2).

It is also clear that the amplitude of the Rayleigh peaks, whose appearance is associated with the excitation of purely surface waves, decreases as the sagittal plane approaches 45° ((110) plane of the crystal). Even very weak Rayleigh peaks in the 37° and 45° planes can be resolved. Their amplitude is 50 to 100 times smaller than the amplitude of the largest of the observed peaks (the amplitude of the left-hand peak in Fig. 7a is more than 0.1; the peak value is cut off by the frame of the plot in order to preserve the same large scale for all six curves).

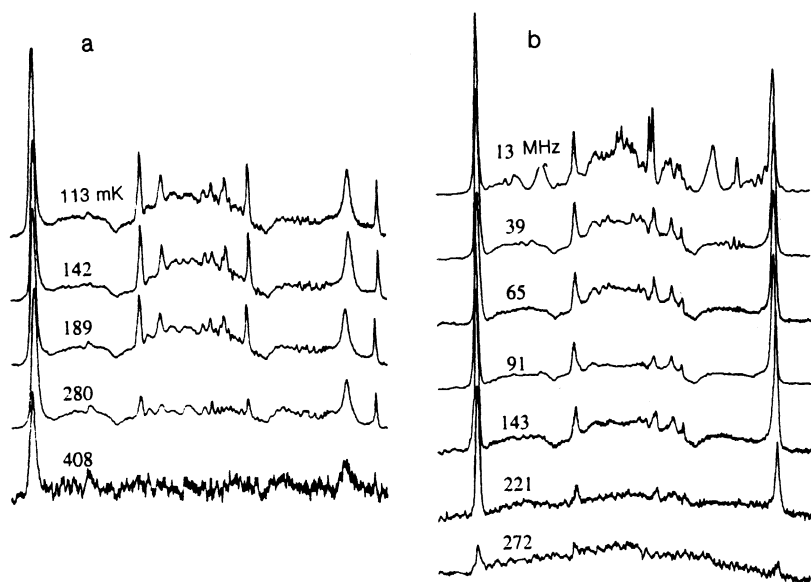


FIG. 8. Experimental spectra of ultrasound transmission into copper in the plane $\varphi=29^\circ$ at $f=38.89$ MHz and different temperatures (a), and in the plane $\varphi=37^\circ$ at $T \approx 140$ mK and different frequencies (b).

Thus far, resonances associated with the excitation of surface modes have been observed only in Refs. 5 and 6 in measurements of phonon transmission through an interface between two media at low temperatures. In the results presented there, the observed height of the peak is only 0.004, i.e., 25 times smaller. The possibility of observing peaks as sharp and high as in the present work is important, for example, as an experimental confirmation of Andreev's theory.³ The latter theory predicts the existence of acoustic resonant transmission peaks with a height of the order of unity (i.e., 200–400 times greater than in the continuum). We have observed peaks 30 times higher than the continuum (Fig. 7a).

Continuum. The region of the continuum falls within the range of angles $-6^\circ < \vartheta < 6^\circ$ and consists of two regions, one where transmission of only transverse phonons is observed, and the region of longitudinal phonons. The transverse phonons lie at the edges of the spectrum in the range $3^\circ < \vartheta < 6^\circ$ and are separated from the region of longitudinal phonons, lying at the center of the spectrum, by pronounced minima in the spectrum. These minima are predicted by the calculations, and their experimental observation indicates that, in accordance with theory, both longitudinal and transverse phonons are indeed excited when longitudinal phonons are transmitted from liquid helium into a solid. The existence of a minimum indicates that both types of phonons are excited in the solid, coherently rather than independently, and their interference can suppress the transmission of acoustic energy.

Thus, the experimental observation of minima is an important confirmation of the applicability of the acoustic theory to the problem at hand. Minima are absent from previously published data.^{5,6}

The continuum contains many stable features that look like noise but are not. Several curves, recorded at different temperatures and frequencies and containing many small reproducible peaks, are presented in Fig. 8.

Some of the grossest features of the continuous spectrum are described by the theory. The calculations predict

the existence of a "bump" at angle of incidence $\vartheta = -5.5^\circ \dots -6.0^\circ$ in Fig. 7b and two peaks (a large peak at $\vartheta = 5.5^\circ$ and a small peak at $\vartheta = 6.0^\circ$) in Fig. 7c and others. Most small peaks are a consequence of the small deviation of the plane of the sample by an angle $\beta = 4.5^\circ$ from the basal plane of the copper single crystal. The deviation is known from x-ray diffraction analysis of the sample, and is taken into account in the construction of all theoretical curves with the exception of the curve in Fig. 10 (see below).

The fact that the theory describes, at least qualitatively, the small features is a strong argument in favor of the theory. It is obvious, however, that the measurements have many details which are not explained by the theory,

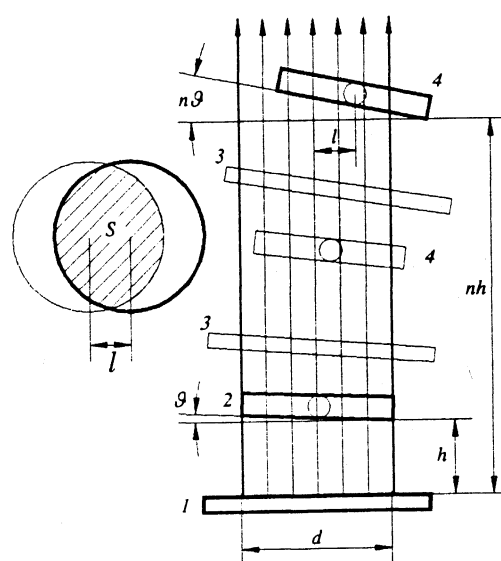


FIG. 9. Geometry of multiple reflections of ultrasound: 1—quartz ultrasound emitter; 2—sample; 3—quartz image in the sample with specular reflection of sound from the surface of the sample; 4—image of the sample in the image of the quartz, etc.

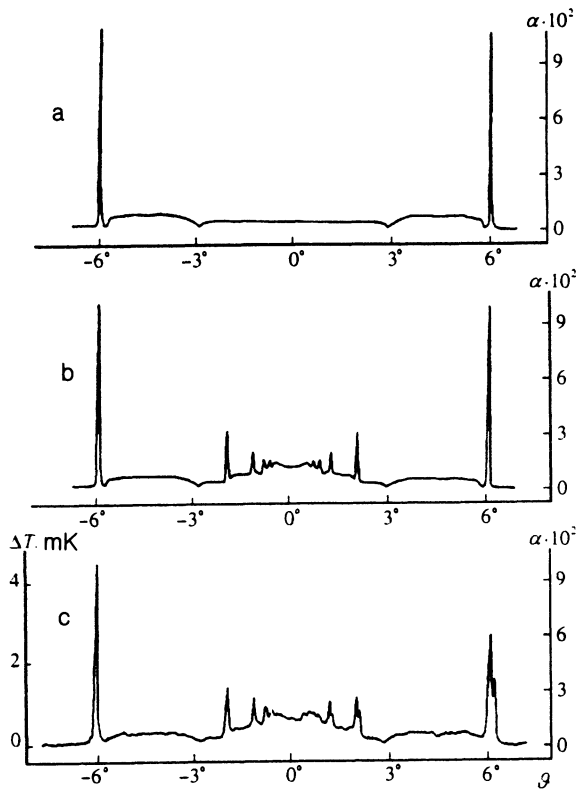


FIG. 10. Angular dependence of the coefficient of transmission of sound energy $\alpha(\vartheta)$ from ${}^4\text{He}$ into a copper single crystal for the (001) plane. Sound is incident in the (100) plane. Curve *a* was computed for a plane wave incident from liquid ${}^4\text{He}$ onto an infinite copper half-space. The damping in copper $p=4 \cdot 10^{-3}$, $\alpha_{\text{RW}}=0.4$, and the resonance width $\delta \approx 1'$. Curve *b* was computed for a fixed geometry taking into account multiple reflections of sound between the sample and quartz, instrumental broadening of the peaks, and sound damping in helium $\gamma=0.15$ dB/cm. Curve *c* is the experimental record of heating ΔT (in mK) of the sample by sound with radiation power $\sim 5 \mu\text{W}$, temperature 107 mK, and frequency 65 MHz. The coefficient $\alpha(\vartheta)$ was obtained from $\Delta T(\vartheta)$ after normalizing at angles of incidence corresponding to excitation of the transverse mode of the oscillations.

and this makes it impossible to conclude at this point in our exposition that the measured spectra correspond to the computed spectra. Since this is a fundamental result, it will be shown below that the discrepancies can be attributed to instrumental effects.

4.4. Reasons for the discrepancies between the measured spectra and the theory

Comparing the experimental curves to the theoretical curves (Fig. 7) shows that several types of systematic differences exist between them.

1. The experimentally measured transmission coefficient $\alpha(\vartheta)$ is significantly greater than the theoretically computed coefficient for angles in the range $-2^\circ < \vartheta < 2^\circ$. A similar effect was also observed previously in Refs. 5 and 6.

2. Many well-resolved peaks that cannot be described by the acoustic theory are also observed in the same region.

3. The experimental data show stable "ripples" on the curves in the region of transverse waves (for example, in the region $4.5^\circ < \vartheta < 5.5^\circ$ in Fig. 7c).

4. Splitting of the resonance is clearly visible on some curves (for example, the right-hand peak in Fig. 7a).

We now analyze these differences and show that they can all be explained by different instrumental effects.

Finite size of the experimental cell. Influence of multiple reflections. Due to the lack of space in the experimental cell, the frame with the sample was placed next to the quartz transducer. The distance between the sample and the quartz is 5 mm. This distance can also not be increased because of considerations of minimum scattering of ultrasound in the liquid at the highest frequencies.

Due to the short distance between the quartz transducer and the sample and the small angles of rotation of the surface of the sample toward the surface of the quartz, multiple reflections of ultrasound occur between them. Ultrasound emitted by the quartz transducer strikes the flat surface of the sample at an angle ϑ and is partially transmitted into the sample, but a large fraction (~ 0.995) of its energy is reflected back and strikes the quartz surface. The ultrasound reflected from the quartz surface once again strikes the sample but this time at an angle of 3ϑ , after which the process repeats. The geometry of multiple reflections of ultrasound is illustrated in Fig. 9. After n reflections (n is any odd number) the image of the sample 4 (thick lines) rotates relative to the direction of propagation of the ultrasound by the total angle $n\vartheta$ and is shifted relative to the axis of the beam by the distance $l=(nh)(n\vartheta)/2$.

Secondary peaks appear in the observed spectrum as a result of multiple reflections of ultrasound. These peaks are associated with the excitation of surface waves when ultrasound strikes the sample after n reflections ($n=3, 5, 7, \dots$ is an odd number). The peak corresponding to n reflections is observed at an angle of rotation of the frame ϑ_{RW}/n , and in the ideal case its width is n times smaller than and its amplitude is the same as the width and amplitude of the main peak.

In the experimental data, however, the width of such peaks is only slightly less than that of the main peak. This indicates that the observed width of the peak is not the natural width, but rather the width of the instrumental function (angular resolution of the detector). The fact that the widths of the secondary peaks are smaller than the width of the main peak is also associated with instrumental broadening.

Since a wave incident within the critical cone is transmitted into the sample with approximately the same amplitude $\alpha \sim 0.005$ for all angles of incidence, the transmission amplitude in the region of the continuum also increases because the energy of the multiply reflected waves adds to the energy of the waves transmitted into the sample. Specifically, the observed transmission amplitude is doubled at angles $\vartheta < \vartheta/3$, tripled in the range $\vartheta < \vartheta/5$, and so on. The latter effect is clearly visible in all experimental curves. This is confirmed well by calculations that take such multiple reflections into account (Fig. 10). As follows from a comparison of the measured spectrum with the theoretical spectrum, the multiple reflection effect also adequately describes the appearance of numerous peaks

near normal incidence of the sound, and the increase in the signal amplitude in this region.

To take the influence of multiple reflections on the measured spectrum into account, it is necessary to take into account the following reasons for attenuation of the amplitude of the wave incident on the sample after n reflections. First, because the image of the sample is displaced away from the beam axis, only a part S of the surface of the sample is exposed, not the entire sample (see Fig. 9). Second, the path of ultrasound in the liquid helium is n times longer, as a result of which the fraction of the scattered ultrasound increases and, correspondingly, the amplitude of the ultrasound reaching the surface of the sample after n reflections decreases. Both attenuation effects were taken into account when the expected pattern displayed in Fig. 10b was constructed.

The attenuation of ultrasound due to scattering in liquid helium is also appreciable in Fig. 8, where it is clear that the signal amplitude at the center decreases with increasing ultrasound frequency and temperature, when the scattering of ultrasound in liquid helium increases. The dependence of the signal amplitude at the center on the ultrasound frequency and the temperature of liquid helium makes it possible, in principle, to measure the sound absorption in liquid helium.

Interference of the waves transmitted into the sample.

In our discussion of the method for measuring the transmission coefficient, we derived Eq. (14) under the assumption that all phonon energy transmitted into the sample is immediately converted into heat. In reality, because the phonon mean free path in the copper single crystal is finite, thermalization process does not occur immediately.

A phonon refracted at the boundary according to Snell's law can propagate up to the back face of the sample and, reflecting from it, once again strike the front face from the opposite direction. The effect produced by the interference of the phonon incident from below with the phonon which has just entered the sample is similar to what happens in a Fabry-Perot interferometer. The difference is that the polarization of the acoustic phonon changes on reflection from the back face of the sample.

The interface between the liquid helium and copper is optically an extremely good mirror with reflection coefficient $r = 1 - \alpha \approx 0.995$, but thanks to the strong scattering of the phonon by the conduction electrons in the volume of the sample, the resulting efficiency of the copper single crystal as an interferometer is low. Nonetheless, at lower frequencies (up to 100 MHz), stable ripples can be seen in the experimental curves in the region of transverse waves (for example, in the region $4.5^\circ < \vartheta < 5.5^\circ$ in Fig. 7c).

As expected, the period of the ripples decreases with increasing frequency of the ultrasound and precisely inversely as the frequency. We calculated specially the interference effect; the results are displayed in Fig. 11. This figure shows the experimental (solid lines) and theoretical (dashed lines) curves of ultrasonic energy transmission into the sample for the propagation direction $\varphi = 22^\circ$ at three different frequencies. The interference of acoustic waves in the volume of the sample was taken into account

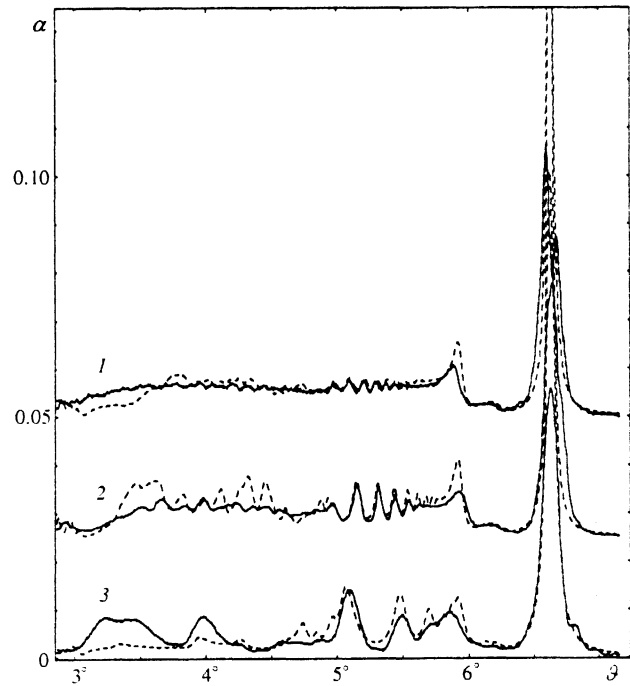


FIG. 11. Influence of the interference of waves transmitted into the sample on the measured spectrum. The experimental (solid lines) and theoretical (dashed lines) curves of the transmission of ultrasound into the sample for directions of propagation $\varphi = 22^\circ$ are presented for three different frequencies. The theoretical curves take into account the interference of acoustic waves in the volume of the sample. The curves were constructed for the following values of the parameters: 1— $f = 64.80$ MHz, $h = 1.45$ mm, $p = 0.006$; 2— $f = 38.89$ MHz, $h = 1.44$ mm, $p = 0.004$; 3— $f = 12.91$ MHz, $h = 1.44$ mm, $p = 0.003$. The measured thickness of the sample is $h = 1.34$ mm.

when the theoretical curves were constructed.

The measured thickness of the sample was $h = 1.34$ mm. The position of the peaks was determined by the phase of the interfering waves, and depends strongly on the thickness of the sample. Since the exact azimuthal direction was unknown, a small adjustment of the thickness of the sample was admissible in all cases. For the same reason, it was impossible to fit the data over the entire range of angles $-6^\circ < \vartheta < 6^\circ$: the phase is disrupted. In addition, the moduli of elasticity of copper, which we took from Ref. 21 for the calculations, are probably not accurate enough.

The value of the absorption coefficient p was chosen in all three cases so as to obtain the best agreement for the interference amplitude. In this case we do not insist that the experimental results agree precisely with the calculations, but only that they show that the "harmonica" of peaks in the region of transverse waves is due to the interference of acoustic waves in the sample.

The following facts also support this result.

1. The position, shape, and amplitude of the peaks making up the interference harmonica do not depend on the temperature. This can be seen in Fig. 8a.

2. The amplitude of the harmonica decreases with increasing frequency (Fig. 8b) because the phonon mean free path decreases. The interference spoils especially strongly the transmission spectrum for 12.91 MHz pho-

nons, where the mean free path equals several thicknesses of the sample.

The interference of sound inside the sample can be used to measure the elastic moduli of the material or, conversely, to monitor accurately the angle of rotation. The advantages of this method would be good accuracy, sensitivity, and stability, which are characteristic of the interference method in general.

Splitting of the resonances. Splitting of the resonance peak is observed in many of the spectra obtained. For example, the right-hand Rayleigh peak in Fig. 7a is split, the angular splitting between the resolved satellites being about $10'$. Analysis of the curves showed that splitting of a peak is stable for a given direction, i.e., the existence of splitting and the distance between the satellites do not depend on the temperature or frequency. Moreover, the peak at $\vartheta = 2^\circ$ in Fig. 7a (from triple reflection) is also split.

The ratio of the heights of the peaks and the resolution of the splitting, however, do depend on the frequency. This is probably connected with the change in the width of the instrumental function, which is minimum at a frequency of the order of 100 MHz. The maximally resolved splitting of a resonance peak is observed at 65 and 91 MHz.

The nature of the splitting of the peaks is still not entirely clear. We considered the following possibilities.

1. A periodic structure formed on the surface of the sample due to electrochemical polishing. A surface wave is scattered by this structure forward/backward, and acquires an additional wave vector equal to the reciprocal period of the structure. This is inconsistent with information about the state of the surface of the sample. Moreover, the angular splitting of the peak would be inversely proportional to the frequency.

2. Surface waves propagating along the front and back face of the sample become hybridized, creating two new modes (symmetric and antisymmetric) separated by a gap—these modes are known as Love waves in thin plates. Since, however, the thickness of the sample is not less than one-tenth of the wavelength and the gap width depends exponentially on the thickness of the plate, this splitting is insufficient to explain the effect. Moreover, Love waves exhibit dispersion, which causes the splitting between the satellites to be frequency dependent.

In our opinion, the splitting of the peaks is most likely due to the mosaic structure of the crystal from the which the sample was prepared. The crystallites are disoriented by an angle of about 2° .

To check this hypothesis, we calculated theoretically the spectrum of transmission of sound into a defective crystal consisting of two crystallites. The same splitting between the satellites as in the experimental records is obtained by assuming that the angle of disorientation of the crystallites equals 3° . Since the disorientation of the crystallites is not determined very accurately from the Laue pattern of the sample, this explanation of the splitting effect can be considered to be satisfactory.

Because copper is highly ductile, the mosaic structure of the single crystals is a very typical defect, if careful measures are not taken to eliminate vibrations, to monitor

the temperature, and so on when the crystals are grown.

5. CONCLUSIONS

Our method for studying the surface modes in the (001) plane of copper consists of measuring the transmission coefficient of the energy of an acoustic wave through the interface between liquid ^4He and copper. This method has the advantage that information about the transmission of acoustic phonons through the boundary can be obtained at the same time that the characteristic surface waves are studied. This is important in studying Kapitza resistance.

When surface waves are excited, the transmission coefficient has a peak of order unity at certain angles of incidence. The height of the peak depends on the dissipation of the surface wave and, within the approximations employed, it is sufficient to have very small scattering (arbitrarily small) for some directions in order for a peak of unit height to exist.

Both purely Rayleigh surface waves and pseudosurface waves were observed experimentally in the (100) plane of the fcc copper crystal.

We were the first to observe in the angular dependences $\alpha(\vartheta)$ two symmetrically disposed minima, corresponding to the first and second critical angles of incidence of sound at the theoretically predicted locations: the first minimum determines the boundary between the volume longitudinal and volume transverse excitations, and the second determines the boundary between the volume and surface excitations of the copper single crystal.

We observed that within $\sim 2^\circ$, the sound energy transmission is higher than the theoretical transmission because of numerous well-resolved weak peaks due to multiple reflections of sound between the sample and the emitter.

We thank A. F. Andreev for discussions of these results and for valuable remarks, and V. N. Krutikhin for assistance in the preparation and conduct of the experiments.

¹From the standpoint of clarifying the nature of the thermal boundary resistance.

²A flop is one floating-point operation.

³To be precise, this should be expressed as follows: the wave vector of the surface wave with a given frequency must be greater than the tangential component of any wave propagating in the solid in the chosen sagittal plane. We shall always assume in the anisotropic case that we are talking about projections of the isofrequency surface on the plane of the boundary. Mentioning this circumstance explicitly makes the phrase very confusing, as in this case.

⁴By polarization we do not mean here the displacement vector of the particles of the body during the passage of the wave. A surface wave, in general, does not have such a vector, since displacements in the wave occur along an ellipse. Polarization should be understood as a collection of vectors (in the general case, imaginary) of displacements and stresses in the wave.

¹ P. L. Kapitza, Zh. Eksp. Teor. Fiz. **11**, 1 (1941).

² I. M. Khalatnikov, Zh. Eksp. Teor. Fiz. **22**, 687 (1952).

³ A. F. Andreev, Zh. Eksp. Teor. Fiz. **43**, 358 (1962) [Sov. Phys. JETP **16**, 257 (1963)].

⁴ A. F. Andreev, Zh. Eksp. Teor. Fiz. **43**, 1535 (1962) [Sov. Phys. JETP **16**, 1084 (1963)].

⁵ K. N. Zinov'eva, Pis'ma Zh. Eksp. Teor. Fiz. **28**, 294 (1978) [JETP Lett. **28**, 269 (1978)].

- ⁶K. N. Zinov'eva, Zh. Eksp. Teor. Fiz. **79**, 1973 (1980) [Sov. Phys. JETP **52**, 996 (1980)].
- ⁷A. G. F. Wyatt, G. J. Page, and R. A. Sherlock, Phys. Rev. Lett. **36**, 1184 (1976).
- ⁸G. N. Crisp, R. A. Sherlock, and A. F. G. Wyatt, in *Phonon Scattering in Solids*, L. J. Challis, V. W. Rampton, and A. F. G. Wyatt (eds.), Plenum, New York (1976).
- ⁹H. Kinder, K. H. Wichert, and C. Hoss, in *Proceedings of the 7th International Conference on Phonon Scattering in Condensed Matter*, M. Meissner and R. O. Pohl (eds.), Springer-Verlag, New York (1992), p. 392.
- ¹⁰T. Nakayama, in *Prog. Low-Temp. Phys.*, Vol. 12, Elsevier, Amsterdam (1989).
- ¹¹E. T. Swartz and R. O. Pohl, Rev. Mod. Phys. **61**, 605 (1989).
- ¹²O. Koblinger, Y. Heim, M. Welte, and W. Eisenmenger, Phys. Rev. Lett. **51**, 284 (1983).
- ¹³J. R. Olson and R. O. Pohl, in *Proceedings of the 7th International Conference on Phonon Scattering in Condensed Matter*, M. Meissner and R. O. Pohl (eds.), Springer-Verlag, New York (1992), p. 399.
- ¹⁴G. W. Farnell, in *Acoustic Surface Waves*, A. A. Oliner (ed.), Springer-Verlag, New York (1978), p. 226.
- ¹⁵Yu. A. Kosevich and E. S. Syркин, Zh. Eksp. Teor. Fiz. **89**, 2221 (1985) [Sov. Phys. JETP **62**, 1282 (1985)].
- ¹⁶L. A. Lyusternik and V. I. Sobolev, *Elements of Functional Analysis* [in Russian], Nauka, Moscow (1965).
- ¹⁷R. Stoneley, Proc. Roy. Soc. A **232**, 447 (1955).
- ¹⁸J. Lothe and D. M. Barnett, J. Appl. Phys. **47**, 428 (1976).
- ¹⁹L. D. Landau and E. M. Lifshitz, *Theory of Elasticity*, Pergamon Press, New York (1987).
- ²⁰R. W. Powers, Electrochem. Tech. **2**, 274 (1964).
- ²¹K. A. E. Goens, Ann. Phys. Chem. **5** 38, 456 (1956).

Translated by M. E. Alferieff